Accepted for publication in Bulletin of the Seismological Society of America, 8th September 2021

Comment on "Activation rate of seismicity for hydraulic fracture wells in the Western Canadian Sedimentary Basin" by Ghofrani and Atkinson (2020)

James P. Verdon[1*], Julian J. Bommer[2]

1. School of Earth Sciences, University of Bristol, Wills Memorial Building, Queen's Road, Bristol, U.K., BS8 1RJ. Orcid: 0000-0002-8410-2703

2. Department of Civil and Environmental Engineering, Imperial College London, Skempton Building, South Kensington, U.K., SW7 2AZ. Orcid: 0000-0002-9709-5223

* Corresponding Author. Email: James.Verdon@bristol.ac.uk, Tel: 0044 117 331 5135.

It is well established that injection of fluids into the subsurface can cause induced seismicity. Cases of injection-induced seismicity have been documented during wastewater disposal, hydraulic fracturing, and geothermal energy production. However, attribution of seismic activity to specific causative activities can be challenging (e.g., Verdon et al., 2019a). It is important to correctly ascertain when and where seismic events have been induced by human activities. In cases where multiple activities take place in the subsurface, it is equally important to ascertain which activities have been responsible for causing induced seismicity.

The correct attribution of induced seismicity has importance both for the appropriate regulation of subsurface industries, and for our scientific understanding of this phenomenon. Establishment of causation has great significance when establishing the seismic risk posed by different types of subsurface activity (and by the same type of activity conducted in different formations or geological settings). Probabilistic assessments of seismic risk are typically driven by extrapolation from past observations of seismicity. Hence, accurate characterisations of observed rates and magnitudes of induced seismicity are required. This issue has enormous implications for livelihoods and for public safety. If seismic events are incorrectly thought to have been induced by a particular activity, when they are in fact natural (or induced by a different activity), then regulators may respond with increased regulatory burdens, or even outright bans, creating a significant impact to the livelihoods of those working in the industry in question, as well as impacting the wider economic benefits that an industry might provide to a particular area. On the other hand, if seismic events are incorrectly characterised as natural when they have in fact been induced, then appropriate mitigation may not be applied where it is necessary, resulting in an increased level of seismic risk that could otherwise have been avoided.

From a scientific perspective, we are increasingly seeing studies that use compilations of induced seismicity cases in order to learn more about the key factors and processes that govern induced seismicity (e.g., Pawley et al., 2018; Igonin and Eaton, 2018; Foulger et al., 2018; Baisch et al., 2019; Verdon and Bommer, 2021). If cases are included in such compilations that are not actually induced, or where the causative activity is incorrectly ascribed, then the learnings that we might otherwise make from such compilations may not be valid.

We are writing this comment to address the estimates made by Ghofrani and Atkinson (2020) (GA20 hereafter) of recurrence rates (i.e., number of cases per stimulated well) of hydraulic fracturing-induced seismicity (HF-IS) as a function of different formations in the Western Canadian Sedimentary Basin (WCSB), with a particular focus on their claims that HF-IS has been caused by operations in shallower formations within the basin, such as the Cretaceous-age Mannville, Cardium and Dunvegan.

In the West Canadian Sedimentary Basin (WCSB), hydraulic fracturing-induced seismicity (HF-IS) has been clearly demonstrated from stimulation of the Upper Devonian Horn River (disaggregated by GA20 into the Muskwa, Evie and Otter Park members) (Farahbod et al., 2015), the Upper Devonian Duvernay (e.g., Bao and Eaton, 2016), and Lower Triassic Montney (e.g., Roth et al., 2020) shale formations.

Cases of induced seismicity in the WCSB have also been identified from wastewater disposal operations in deep formations (e.g., Schultz et al., 2014; Anderson and Eaton, 2016; Hosseini and Eaton, 2018), and from conventional hydrocarbon operations (e.g., Wetmiller, 1986; Baranova et al., 1999), although it is by no means clear whether the seismicity at Rocky Mountain House is in fact generated by conventional production or by co-located wastewater injection into underlying formations.

The cases of induced seismicity in the above-referenced studies were all caused by hydrocarbon operations in Palaeozoic or lower Mesozoic formations. GA20 is the first study that we are aware of that has presented a claim for HF-IS in the WCSB having been caused by operations targeting shallower formations situated above the lower-Cretaceous unconformity. This major, basin-wide unconformity separates carbonate-

dominated Palaeozoic (and lower Mesozoic) sediments, deposited on a passive extensional/trans-tensional margin, from the clastic-dominated Cretaceous and Cenozoic-age sediments deposited in a foreland basin created by uplift of the sierras to the west and south (Mossop and Shetsen, 1994). The shallower formations being targeted in the Cretaceous section are, broadly speaking, tight sandstone plays rather than shale formations. It is not disputed that hydraulic fracturing and wastewater disposal in Palaeozoic formations has generated induced seismicity with magnitudes M > 3. However, GA20 claim that the rates of seismicity generated by hydraulic fracturing in the Dunvegan and Gething formations (association percentage of 0.7 % at W > 0.35, Table 2 of GA20) are of a similar order of magnitude to the rate at which the Montney formation has generated induced seismicity (association percentage of 1.5 % at W > 0.35), and that seismicity has also been generated by stimulation of the Cardium and Mannville formations.

The method used by GA20 uses extremely loose spatiotemporal criteria to assign induced seismicity associations, and it fails to consider the impacts of the overlap that exists between different types of operation within the WCSB. As a result, the links made by GA20 between seismicity and hydraulic stimulation of shallower formations in the WCSB are erroneous.

THE GHOFRANI AND ATKINSON (2020) METHOD

There is a growing body of literature that describes how seismicity can be assessed as being natural or induced, and if induced, by which activity (e.g., Davis and Frohlich, 1993; Davis et al., 1995; Cesca et al., 2012; Dahm et al., 2013; Passarelli et al., 2013; Oprsal and Eisner, 2014; Dahm et al., 2015; Goebel et al., 2015; Schoenball et al., 2015; Frohlich et al., 2016; Verdon et al., 2019a). The waveforms generated by induced earthquakes are not significantly different from those generated by natural earthquakes. As such, causation is usually established via considerations of temporal correlation between seismicity and the activity in question, spatial proximity (both laterally and, where earthquake depths are constrained, in depth), precedent and past rates of activity (both of natural seismicity rates and of seismicity generated by similar industrial activities), and considerations of whether the activity in question could have created a hydraulic or geomechanical perturbation at the earthquake hypocentre of sufficient size and mechanism to have triggered the event.

It is notable that GA20 do not engage with any of the approaches proposed in these studies. The GA20 method is based solely on spatiotemporal coincidence, where values are assigned to a parameter, W, on the basis of separation between the HF well pad and earthquake epicentre (taking a value of 1 for distances ≤ 3 km) and of time after the start of the hydraulic fracturing (taking a value of 1 for intervals of 5 days or less); the final value of W, which indicates the likelihood of association, is the average of the two values determined from the windows of distance and time. A value of W = 0.35, the level described by GA20 "as passing a reasonable threshold for association" could be obtained, for example, by an earthquake occurring at 20 km from a hydraulically fractured well within 10 days of stimulation, or by an earthquake occurring at 4.5 km from a well within 90 days of stimulation. A value of W = 0.5 (the highest level in Table 2 of GA20) could be obtained by an event that is 20 km from a well within 5.7 days of stimulation, or at 3.3 km from a well within 90 days of stimulation. A striking aspect of the nature of GA20's method of calculating W via an arithmetic mean of the spatial and temporal weightings is that a value of W = 0.5 can be obtained even when one of the weighting factors (W_T or W_D) is equal to zero. In other words, an association between the earthquake and a specific well can be inferred despite being scored as impossible in terms of either space or time.

We also note in passing that, while GA20 describe W ≥ 0.35 as "a reasonable threshold for association", they later argue that results from W ≥ 0.25 are statistically significant. In their Table 2, GA20 include

association rates from W values down to $W \geq 0.15$, and events with $W \geq 0.15$ are included in their Table A1 of associated events, producing a potential ambiguity for the reader with respect to an appropriate W value for potential association.

Irregardless of the choice of W threshold, the criteria for spatiotemporal coincidence used by GA20 are remarkably loose. Verdon and Bommer (2021) investigated the temporal evolution of HF-IS from case studies around the world. If an induced event were to occur after the end of stimulation, when no seismicity had been recorded during operations, a post-injection increase in magnitude would have occurred. The largest time-lag observed between the end of hydraulic fracturing and an increase in seismic magnitudes was 23 days (Verdon and Bommer, 2021). Hence, the 90-day window allowed by GA20 (a time lag with which an event could still score a W value as high as 0.5) is almost 4 times larger than the longest lag ever observed for a case of HF-IS.

Similarly, where high-resolution local monitoring networks have been used to monitor HF-IS, events locations are found to be at most within 1 – 2 km of the causative well (e.g., Bao and Eaton, 2016; Eaton et al., 2018; Kettlety et al., 2019; Clarke et al., 2019; Kettlety et al., 2020a,b). GA20 argue for the larger distances allowed by their W parameter based on event location uncertainties and the use of horizontal drilling. However, the publicly available database of stimulated wells provided by the Alberta Energy Regulator includes both surface and well-bottom coordinates, so it is possible to explicitly include deviated wells in any assessment of spatio-temporal co-incidence.

GA20 claim that the typical location uncertainty of catalog events in the WCSB is approximately 10 km. Their estimate is based on discrepancies in epicentral locations quoted by different monitoring agencies. This is not an appropriate way to determine location uncertainties where different networks are used to locate the same event. A discrepancy in event location might be expected if one agency (such as the Alberta Geological Survey, AGS) was using a denser, regional network while another (the Canadian National Seismograph Network, CNSN, for example) was using a more sparse, national monitoring network. Any location discrepancies would reflect the larger uncertainties in the lower resolution network, and they would not define the precision of the denser-resolution network. Schultz et al. (2015) performed an assessment of the AGS seismic network capability and found location uncertainties typically ranging from $< 1 – 3$ km for $M \geq 3.0$ events across much of the area of interest where oilfield activities are taking place in Alberta.

Given that location uncertainties are expected to be within 3 km, and that events are generally found to occur within 2 km of a causative well when high quality local monitoring is available, a maximum distance of 5 km from any part of the subsurface well track might be a more suitable cut-off.

A more significant shortcoming of the GA20 approach is that no other potential anthropogenic causes were considered. As described above, it is well established that induced seismicity in the WCSB has been caused by hydraulic fracturing in the Duvernay, Montney and Horn River shale formations, and by wastewater disposal in certain formations. When associating induced seismicity with other activities, such as hydraulic fracturing in shallower formations, the dominant seismicity signal from the known seismogenic activities must first be accounted for. Otherwise, the GA20 method could still associate an event with a relatively weak W score with a given well, when in fact there is a far more clear and obvious cause. In fact, the most obvious utility of the GA20 approach would be to use relative W scores for different subsurface activities around the same earthquake to establish the most likely cause of an event.

GA20 use a Monte Carlo simulation to assess the statistical significance of their results. A Monte Carlo simulation would be a valid way of assessing statistical significance if the null hypothesis was that earthquakes were occurring randomly. This would be a reasonable assumption for a comparison with natural earthquake genesis. However, it is well established that hydraulic fracturing in the Horn River,

Montney and Duvernay shales, and wastewater disposal in deeper formations, has driven much of the seismicity observed in the WCSB over the last few decades. As a result, the occurrence of seismicity is not random, but will occur in spatial and temporal correlation with these activities, and so random earthquake genesis is not an appropriate null hypothesis when assessing whether hydraulic fracturing in shallower formations has also caused induced seismicity. Hydraulic fracturing wells in shallower formations will have a much higher chance of being linked to earthquakes using the GA20 method where they are found in proximity to the deeper Duvernay, Montney or Horn River wells, or seismogenic waste disposal wells, but this association will be coincidental.

Thus, GA20 have used a Monte Carlo simulation to examine the ability of the W parameter to discriminate between induced and natural events. However, they have not tested its ability to discriminate between different potential causes of induced seismicity, which is the key conclusion of the GA20 study, over and above the findings of Atkinson et al. (2016). As such, their conclusions regarding rates at which induced seismicity has been triggered in different formations in the WCSB are not supported by the modelling that they have presented. Consequently, these association rates cannot be used to characterise how often shallower wells generate induced seismicity (or indeed whether they generate any induced seismicity at all).

RE-ASSESSMENT OF GHOFRANI AND ATKINSON (2020) CASES

GA20 argue that their model is probabilistic, and that while some false positives will be generated by their loose spatio-temporal criteria, their use of summed W values will account for the false positives. The validity of their approach is based on a top-down assessment of the association rates that are produced – that they are similar to previous rates found by Atkinson et al. (2016). We note that Atkinson et al. (2016) used similar criteria in their assessment, and the fact that similar methods produce similar results is a circular argument, and not, in and of itself, a validation of the method.

More importantly, a bottom-up assessment of the credibility of their method is also possible. There remains a deterministic element to the GA20 approach, since their results present a description of what has happened – they are not a forecast of what might happen going forward. Their approach associates specific earthquakes with specific hydraulic fracturing wells in order to calculate rates of induced earthquakes above a certain magnitude per well, and as such it is possible to examine each case in detail to investigate whether the potential association is credible.

For wells targeting Cretaceous-age formations (Cardium, Dunvegan, Gething, Cadomin, Glauconitic Sandstone, Basal Belly River Sandstone, as per GA20 Table 2), GA20 identify only 11 wells at the $W \geq 0.35$ level. This is a very small population of cases with which to make any probabilistic assessment of results. When performing any top-down assessment of the statistical results, this small number of cases will be lost among the hundreds of cases of induced seismicity generated by the Montney and Duvernay formations (which we agree have generated HF-IS at high rates).

For the small number of cases in Cretaceous-age formations, it is far more appropriate to perform a bottom-up assessment, where the validity of each individual event and well can be examined on a case-by-case basis to evaluate whether the association proposed by GA20 is credible. In the following section (and continued in our Appendix) we adopt this approach, examining in detail every single case where an association with $W \geq 0.35$ between an $M \geq 3.0$ event and a hydraulically fractured well targeting Cretaceous-age formations could be found.

GA20 did not specify which events they linked to which specific wells targeting Cretaceous-age formations. This critical information, specifying which $M \geq 3.0$ events are linked to which specific wells that make up the Cretaceous formation cases in GA20 Table 2 has not been provided. Therefore, to assess events on a case-by-case basis, we have repeated GA20's analysis. Following GA20, we used $M \geq 3.0$ earthquakes listed in the Composite Alberta Seismicity Catalog from 2009 – April 2019, and the well database provided by the Alberta Energy Regulator. Table 1 lists all earthquakes that we have identified as having $W \geq 0.35$ when paired with a well targeting a formation of Cretaceous age. In total, we identified 25 $W \geq 0.35$ pairs, corresponding to 9 unique earthquakes, and 17 unique wells. We plot the distribution of well-event distances and time lags in Figure 1, and a map of identified events in Figure 2 (in these figures and tables we refer to all wells targeting members of Mannville age (Aptian/early Albian), including the Fahler; Ostracod Beds; Cadomin; Glauconitic Sand; Bluesky; Gething; Spirit River; Wilrich; Notikewin; Ellerslie, as "Mannville"). Since GA20 did not specify which earthquakes they have associated with which wells, it is not possible to confirm that the cases in Table 1 correspond exactly to the cases identified by GA20, but we have identified similar numbers of events within the different Cretaceous formations as GA20 (as per their Table 2), with similar distributions of W values, indicating that we have very likely identified the same cases.

In the following, we examine these cases in more detail, highlighting how they demonstrate the flaws in the GA20 approach that we described above. In Appendix A we provide a commentary for every case listed in Table 1, which likely represent the entire population of events that have been "associated" by the GA20 method with hydraulic fracturing of Cretaceous-age formations in the WCSB. GA20 accept that their method will produce some false positives. Therefore, the fact that we have examined every single case where $M \geq 3.0$ seismicity has been supposedly linked to hydraulic fracturing of Cretaceous wells, as identified by the GA20 method, is of significance, since we find that all of the identified cases are clearly false positives, and as such there are no cases where hydraulic fracturing of Cretaceous-age formations can be credibly linked to induced earthquakes with $M \geq 3.0$.

Fox Creek Duvernay: 05/12/2017 M3.1; 07/12/2017 M3.1; 16/12/2017 M3.4

This cluster of three $M \geq 3.0$ earthquakes in the Fox Creek region, which occurred over a period of 11 days, was linked by the GA20 method to hydraulic fracturing in one Cardium well (100/12-18-060-17W5/00), five Dunvegan wells (100/05-05-061-18W5/00; 100/13-32-060-18W5/00; 102/03-26-060-18W5/00; 100/04-08-060-17W5/00; 100/05-08-060-17W5/00), and one Viking well (100/03-10-060-17W5/03). However, in the Fox Creek area, induced seismicity has been extensively linked to hydraulic fracturing of the Duvernay formation (e.g., Bao and Eaton, 2016).

Figure 3 shows a map of these events and their relationship to nearby wells. We observe that the events are co-located with a pad of 4 hydraulic fracturing wells (102/06-28-060-18W5/00 100/05-28-060-18W5/00; 100/04-09-061-18W5/00; 102/03-09-061-18W5/00), all of which targeted the Duvernay formation. Each of these wells injected roughly 40,000 m^3 of fluid from late November 2017 to early January 2018, and so stimulation in the Duvernay was active and ongoing when the events occurred. Two other events with $M < 3$ were also co-located with these wells while stimulation was ongoing. The largest W value calculated by GA20 for these events for the Duvernay wells is 0.81, although, since hydraulic fracturing in these wells took place over several weeks, stimulation was ongoing in the Duvernay wells when the events occurred, and so a W value of 1.0 would be appropriate.

The events are more than 5 km from the nearest point of the Cardium well (100/12-18-060-17W5/00) track. This well only injected 3,000 m^3, and stimulation finished on 28th of November, 7 days before the first event in the sequence began. The W values for each of the three events when linked to this well are

0.39, 0.29, and 0.42. The events are more than 10 km from the Viking well, which only injected approximately 100 m^3, on the 10th December, after the sequence of events had initiated.

Three of the Dunvegan wells (100/05-05-061-18W5/00, 100/13-32-060-18W5/00 and 102/03-26-060-18W5/00) are relatively close to the event sequence. Each of these wells injected approximately 3,000 m^3 of fluid, with stimulation lasting only one day per well, conducted for the different wells on 20/10/2017, 18/11/2017 and 19/11/2017 (57, 29 and 28 days before the largest event on 16/12/2017). As discussed above, a time lag of 4 weeks or more between the end of hydraulic fracturing and an increase in event magnitudes would represent a longer lag than has ever been observed in any case study, suggesting that these wells acting as a cause for these events is extremely unlikely.

Two of the Dunvegan wells (100/04-08-060-17W5/00 and 100/05-08-060-17W5/00) were stimulated on the 14th and 16th of December, injecting approximately 3,000 and 5,000 m^3. Hence, these wells had not been stimulated at the time that the sequence of events began. The nearest point of these wells is located over 8 km from the event locations.

The co-location of events with the Duvernay wells, the fact that these Duvernay wells each injected an order of magnitude more fluid than the Cardium and Dunvegan wells, and the fact that the events occurred during stimulation of the Duvernay wells, provides a strong argument that these events were induced by the Duvernay hydraulic fracturing. This is reflected in the high W score for the Duvernay wells. However, these events also score $W > 0.35$ for the wells targeting the Cretaceous-age formations, and so would have been included in the GA20 summation to determine the rates at which Cretaceous formations produce HF-IS.

The events occur weeks after stimulation of the Dunvegan 100/05-05-061-18W5/00, 100/13-32-060-18W5/00 and 102/03-26-060-18W5/00 wells, and are not co-located with the Cardium, Viking, or with the Dunvegan wells 100/04-08-060-17W5/00 and 100/05-08-060-17W5/00. Furthermore, these shallow wells injected an order-of-magnitude less fluid than the Duvernay wells. Hence, we conclude that any links between the events and these Cretaceous wells are extremely weak. It is abundantly clear that these events were induced by hydraulic fracturing in the Duvernay, and therefore would have been erroneously included in the summation used by GA20 to estimate activity rates in Cretaceous formations.

We note that the "W" values for the Dunvegan wells ranged between $0.55 < W < 0.7$. These high values for the Dunvegan wells, despite the clear and obvious lack of causation between these wells and the events, demonstrates that even relatively high W values cannot be taken as providing grounds for linking specific wells with specific earthquakes, unless further quality control assessments are undertaken.

We also note that the event epicenters are all located within 1 – 2 km of the Duvernay wells. The tight co-location between the events and the causative wells lends further evidence to the fact that location uncertainties for most events in the catalog are relatively small, within the range <1 – 3 km estimated by Schultz et al. (2015) for the AGS earthquake catalog in this region.

Finally, the summed W scores for these events highlight a further flaw with the GA20 method. If one includes only Cretaceous wells, the summed W score for the largest of these events is 3.83. While GA20 avoided double-counting wells in their assessment of association percentages (GA20, Table 2), they appear to be double-counting the same earthquake for multiple wells, such that one earthquake that occurred would be allowed to add up to almost 4 earthquakes in the association percentages.

Cordel: 01/01/2013 M 3.0

The GA20 method links a single earthquake within the Cordel cluster to a Cardium well (102/10-09-044-15W5/00), with W = 0.57. The seismicity in the Cordel cluster has been analysed by Schultz et al. (2014), who concluded that these events were triggered by a high-volume water disposal well that is injecting into the Elkton Formation (Mississippian age).

Figure 4 shows a map of this event, and its relationship to adjacent oil and gas activities. Over 70 events with $M \geq 2$ have been identified within the Cordel cluster. The onset of these events began in the early 1990s, after injection began in the 100/10-25-043-16W5/00 well and has continued to date. The event on 01/01/2013 is found within this cluster. The associated Cardium well is 3 km from the event. However, stimulation in this well ceased on 09/12/2012, 23 days before the event occurred. If this event was caused by the Cardium well it would match the longest ever delay observed between the end of a HF operation and an increase in induced event magnitude. More importantly, of the 13 $M \geq 3.0$ events identified in the Cordel cluster, this is the only one that has any spatiotemporal match to any of the nearby hydraulic fracturing wells. In contrast, Schultz et al. (2014) found that the correlation between injection rates in the 100/10-25-043-16W5/00 wastewater disposal well and the Cordel seismicity was statistically significant at a confidence level of 99 %. It is not credible to claim that all other events in this cluster were driven by waste-water disposal, but that this single event was induced by hydraulic fracturing. As such, the association identified by the GA20 method is not plausible.

Ferrier: 10/03/2019 M 3.8

This earthquake is the largest to have been linked by the GA20 method to hydraulic fracturing of a well in Cretaceous-age strata. The GA20 method associates this event with two co-located Cardium wells (104/12-35-042-08W5/00 and 102/13-35-042-08W5/02). These wells both injected approximately 5,000 m^3, from 01/03/2019 to 12/03/2019.

Figure 5 shows a map of this event and nearby oil and gas activities. As with the previous case, several hundred wells have been stimulated in Cretaceous strata within the area shown in Figure 5, and yet this is the only case where stimulation has been linked by the GA20 method to an $M \geq 3.0$ earthquake.

The identified event is over 16 km from the linked wells. A location error far larger than 3 km (as estimated by Schultz et al., 2015), and indeed larger than the 10 km location uncertainties adopted by GA20, would be required to co-locate this event with these wells. This event has a magnitude of M 3.8, and occurs at a relatively central position within the AGS array, and so location uncertainties will be far smaller than this. The distance between this event and the identified wells means that any causative links are not plausible.

The event is located near to the Ferrier field, where a waterflood is being conducted for secondary recovery of conventional resources. Given the proximity of the location, this activity could be a more plausible cause for this event. However, the event hypocentre is located at 14 km depth. Given the event's larger magnitude, and its location within the AGS array, the depth uncertainties are relatively low – the depth uncertainty for this event in the AGS catalog is listed as being ± 2 km. As such, the event depth is very likely to be more than 10 km, and therefore too deep to have been caused by oilfield activities. An M 1.9 aftershock event that occurred later the same day had a similar location depth, indicating that this hypocentral location is robust. Whether or not the event has been caused by the waterflood in the Ferrier field, or is a natural event, it is certainly clear that this event has not been caused by hydraulic fracturing in the Cardium wells over 15 km to the northeast, and that the link implied by the GA20 method is erroneous.

Summary of Observations

In Appendix A we provide similar commentaries for all the events listed in Table 1. In every case, a causative link between the identified events and the wells to which the GA20 method links them is not plausible or credible. Identified events can be clearly linked to hydraulic fracturing of the Duvernay Formation and to sequences of seismicity induced by wastewater disposal, and in some cases events are likely to have a natural origin. We conclude that the associations made by GA20 linking seismicity to hydraulic fracturing in shallow, Cretaceous-age formations are all erroneous. When examining the cases identified using the GA20 method, we are unable to identify any cases where $M \geq 3.0$ earthquakes have been caused by hydraulic fracturing of wells targeting Cretaceous-age strata in the WCSB, with over 10,000 such operations conducted over the past 2 decades.

DISCUSSION

The observations we have presented here merit further discussion with respect to the underlying structural geology and reservoir characteristics that may account for the different HF-IS response between the Duvernay/Horn River/Montney shales and shallower formations. Similar observations with respect to the very different levels of response between different formations at different depths in the same basin have been made in the Appalachian Basin, where the shallower Marcellus Shale has not generated HF-IS, but cases have been recorded from the underlying Utica Shale (Skoumal et al., 2018), and in the UK, where hydraulic fracturing in the Bowland Shale has generated HF-IS (e.g., Clarke et al., 2019; Kettlety et al., 2020b), but stimulation in shallower conventional formations has not (Mustanen et al., 2017).

We note that, for HF-IS to occur, pre-existing faults must be present that are well-orientated in the in situ stress field, with the stress field having sufficient levels of shear stress (high stress anisotropy) such that faults are close to the Mohr-Coulomb failure surface (i.e., they are critically stressed). Furthermore, the hydraulic fracturing must create a perturbation of sufficient size to be capable of reactivating a nearby fault. These criteria should inform explanations of why different formations have, or have not, generated induced seismicity.

Structural Geology

As described in our introduction, the base of the Cretaceous represents a major, basin-wide unconformity in the WCSB, with strata sub-cropping against this surface ranging in age from Devonian to Jurassic (Mossop and Shetsen, 1994). The Palaeozoic succession was deposited on an extensional/trans-tensional passive margin, with sediments sourced from the Canadian Shield to the northeast. The Cretaceous and Cenozoic succession was deposited in a foreland basin created by the uplift of sierras to the southwest, with sediments being sourced from that direction.

Given the different tectonic settings, it might be expected that few geological structures within the Palaeozoic would extend across the base-Cretaceous unconformity, and that there would be much greater potential for activities in the Palaeozoic rocks to impact basement-seated structures. This is found to be the case in practice. Ross and Eaton (1999) compared structures found in the basement to features in the overlying sedimentary sequences, and in general they did not find a strong relationship between the two. In the cases where basement seated structures were observed extending into the overlying sediments, they were not found to extend any shallower than the lower Palaeozoic.

Similar observations have been made using a combination of reflection seismic imaging and microseismic monitoring from cases of HF-IS caused by stimulation of the Duvernay around Fox Creek (Eaton et al.,

2018; Eyre et al., 2019). These observations have revealed fault reactivation on structures that have grown from basement-seated trans-tensional faults that run through the Devonian section, terminating in the Wabamun Formation (Famennian age). Schultz and Wang (2020) have described similar observations during HF-IS cases around Red Deer, concluding that "*hypocentre depths support a conceptual understanding of basement rooted faulting that extends just into the strata overlying the Duvernay Formation*".

These structural conditions may explain why hydraulic fracturing in the Duvernay has generated cases of HF-IS with $M \geq 3.0$, but stimulation of the overlying Cretaceous formations has not. We note that, even in the Fox Creek region, a significant number of wells have been stimulated in Cretaceous formations without generating any HF-IS. This shows that, even in a region that has experienced some of the highest levels of HF induced seismicity in the entire WCSB, the fact that the basement-seated faults, which have been the cause of induced seismicity triggered by Duvernay stimulation, do not extend above the lower Cretaceous unconformity is likely to be a key factor in explaining why the shallower formations have not generated HF-IS.

The geological and structural setting in the region where the Montney formation has generated induced seismicity is substantially different to that around Fox Creek and Red Deer. Much of the HF-IS caused by stimulation of the Montney Shale has taken place within the fold-and-thrust best generated by the Laramide orogeny, and within the Peace River arch. Within the Peace River Arch, the pre-Cambrian basement is significantly uplifted (Mossop and Shetsen, 1994), and there is a higher abundance of trans-tensional faulting extending from the basement. The compressional deformation associated with the Laramide orogeny has generated large NNW-SSE-trending thrust faults observable in reflection seismic datasets (e.g., Riazi et al., 2020). These faults generally extend downward into Palaeozoic strata, and upwards into the Cretaceous section. It is on these thrust faults that induced seismicity in the Montney formation is observed to occur (e.g., Peña Castro et al., 2020; Riazi et al., 2020).

However, within the region where hydraulic fracturing of the Montney has generated HF-IS, very little hydraulic fracturing has taken place in Cretaceous strata (see Figure 2). Some hydraulic fracturing has taken place in the Cadomin (Early Cretaceous) Formation in the Septimus/Dawson area to the southeast of Fort St. John. Injection volumes in these wells are typically insignificant (c. 500 m^3 per well) relative to those used to stimulate the Montney Formation (typically > 10,000 m^3 per well), which represents the predominant activity in this area. $W \geq 0.35$ scores can be obtained for some events with magnitudes ranging from $2.0 < M < 3.0$ and Cadomin wells in this area from July 2017. However, Roth et al. (2020) have analysed this sequence in detail, using local seismometer networks to obtain an event catalog with high precision event locations that is complete to approximately magnitude 1, and comparing this catalog with detailed injection records. Their results provide compelling evidence that the events are closely linked, in both space and time, to high volume hydraulic fracturing activities in the Montney Formation, and any apparent links to low-volume Cadomin activities are clearly co-incidental. Much like the cases we have discussed in the preceding section, this example showcases the pitfalls of relying solely on loose spatio-temporal criteria without examining in detail both the nature of different industrial activities, and the full evolution of induced seismicity sequences.

Overall, however, the conditions that pertain to the Montney within the Laramide fold-and-thrust belt and Peace River Arch do not provide a good analog for the regions further to the southeast where the majority of hydraulic fracturing within Cretaceous formations has taken place.

Reservoir Characteristics and Operational Parameters

The terms employed to characterise "unconventional" hydrocarbon development are often used loosely. Hydraulic fracturing is used to stimulate "shale" reservoirs, and it is also used to stimulate "tight sandstone" reservoirs, where the differentiation between these terms can be based both on the proportion of fine-grained clastic material, and also on the formation permeability.

The three formations that have generated HF-IS with $M \geq 3.0$ in the WCSB can be considered to be shale formations, with typical permeabilities lying in the range 1×10^{-7} to 1×10^{-4} mD (e.g., Chalmers et al., 2012a,b; Yassin et al., 2017; Cui and Nassichuk, 2018; Ghanizadeh et al., 2018). In contrast, most of the key unconventional reservoirs in the Cretaceous section, such as the Cardium, Mannville, and Dunvegan, would be better characterised as tight sandstones, with permeabilities lying in the range 0.01 to 100 mD (e.g., Arndt, 2017; Friesen et al., 2017; Ghanbari et al., 2019).

The higher permeabilities of these formations may have a direct impact on the nature of the perturbation caused by hydraulic fracturing. Intuitively, it might be expected that a higher permeability might allow for hydraulic perturbations to travel further. However, Verdon et al. (2019b) showed how, for HF-IS in the Duvernay formation, the presence of pre-existing fracture corridors provided permeable pathways for fluid pressures to be transferred across a distance of approximately 1 km to reactivate a fault. In the case described by Verdon et al. (2019b), pressures could be transferred over such distances because the rock matrix permeability outside of the fracture corridor was low. If the rock matrix permeability (and porosity) were higher, elevated pressures created by the hydraulic fracturing would be able to quickly dissipate into the matrix pore space, reducing the extent of the perturbation, and therefore reducing the likelihood of fault activation.

The reservoir permeability also determines the scale of hydraulic fracturing operation needed to generate commercial hydrocarbon production rates. Very low permeability shale plays require high volume stimulation, whereas the volumes used to stimulate tight sandstone reservoirs are smaller. Figure 6 shows the injection volumes used per well to stimulate the Cardium, Mannville, Dunvegan, Montney, Duvernay and Horn River formations. For the shale formations, the mean per-well stimulation volumes are 54,000 m^3 for the Horn River, 42,000 m^3 for the Duvernay, and 14,000 m^3 for the Montney. In contrast, for the Cretaceous tight sandstone formations, the mean per-well stimulation volumes are 3,100 m^3 for the Mannville, 2,500 m^3 for the Cardium, and 1,900 m^3 for the Dunvegan. It is well established that rates and magnitudes of induced seismicity scale with injection volume (e.g., Shapiro et al., 2010; McGarr, 2014; van der Elst et al., 2016; Schultz et al., 2018; Verdon and Budge, 2018), and so it is possible that the lower volumes used for hydraulic fracturing in the shallower tight sandstone formations in the WCSB accounts for the absence of $M \geq 3.0$ HF-IS observed for these formations.

It is beyond the scope of this comment to definitively establish why the Cretaceous-age tight gas formations in the WCSB have not generated any induced seismicity with $M \geq 3.0$, while the deeper shale gas formations have – as described above, there are several plausible explanations that include the structural geology of the WCSB, the reservoir characteristics of the different formations, and the nature of the operations that are carried out. In addition, we have not examined the different states of stress that are present in the different formations, since public data with which to fully constrain spatial variations in the in situ effective stress tensor are limited. However, this could be another fruitful avenue of investigation since stress conditions are likely to be higher in deeper formations – Eaton and Schultz (2018) have shown that the occurrence of HF-IS seismicity in the Montney and Duvernay correlates with regions that are significantly overpressured, and Kettlety et al. (2020b) have directly shown how the *in situ* stress conditions can control the extent to which faults can be reactivated by hydraulic fracturing.

At a more general level, it is worth noting that hydraulic fracturing has been used to stimulate conventional and tight reservoirs for many decades, without producing any notable cases of induced seismicity. This led the US National Research Council (2013) to conclude that hydraulic fracturing "*does not pose a high risk for inducing felt seismic events*". All of the cases of HF-IS that have been observed since the National Research Council (2013)'s assessment have been caused by stimulation of shale formations (see Verdon and Bommer, 2021, for a list of case studies). In contrast, we are not aware of any significant cases of HF-IS being generated by stimulation of tight-gas sandstones. Future research might be usefully directed to developing a better understanding of why stimulation of tight sandstones, versus stimulation of certain shale gas plays, has generated such different levels and rates of induced seismicity.

CONCLUSIONS

GA20 have performed an assessment of the rates of induced seismicity generated by stimulation of different formations in the WCSB. They have done so on the basis of remarkably loose spatiotemporal co-incidence criteria. Moreover, since it is well established that seismicity has been caused by hydraulic fracturing in the Horn River, Montney and Duvernay formations, and by wastewater disposal, any attempt to link seismicity to other activities in addition to these established causes must first account for this dominant signal. GA20 use a Monte Carlo simulation to assess the statistical significance of their result. The null hypothesis in their approach is random earthquake occurrence. While this may be a suitable way to discriminate between natural and induced seismicity, it is not suitable for discriminating between different causes of induced seismicity, since in such a scenario, the occurrence of earthquakes is not random. Because many Duvernay and Montney wells have generated induced events, any well that targeted shallower Cretaceous formations where operations in the Duvernay or Montney (or wastewater disposal in deep formations) were also ongoing nearby would have a much higher than random chance of being temporally and spatially coincident with an earthquake. However, this would not indicate that the event and the shallower well were linked in any way, unless further, detailed analysis were to provide evidence of such a link.

We have re-evaluated every single case identified by the GA20 method where hydraulic fracturing in shallower formations (above the lower Cretaceous unconformity) has been linked to an $M \geq 3.0$ seismic event. In all the cases identified, we find that there is no plausible or credible evidence to link events with hydraulic fracturing in Cretaceous strata. Our findings are consistent with the literature on HF-IS in the WCSB to date, where no cases of induced seismicity generated by stimulation of Cretaceous strata have been described.

We have identified sound reasons to account for the different induced seismicity responses between deeper, seismogenic formations in the WCSB, and the shallower formations that have not generated any induced seismicity. These reasons include the different structural geological settings of the different formations, their different reservoir properties, and the different scales of hydraulic fracturing operations typically deployed in them. If induced earthquakes are incorrectly ascribed to activities that did not in fact cause them, then we will limit our ability to correctly identify the different factors that promote or inhibit induced seismicity. Similarly, if we incorrectly ascribe induced events to activities that did not cause them, then our assessments of the seismic hazard associated with these activities will be exaggerated, potentially resulting in the implementation of regulations or mitigating actions that are inappropriate and not needed.

Data and Resources

The earthquake database used for this study was taken from the Composite Seismicity Catalog for Alberta and British Colombia, available at www.inducedseismicity.ca (last accessed September 2020). The hydraulic fracturing and waste disposal well database used for this analysis comes from the Alberta Energy Regulator (AER) Geologic Data Centre.

Statement of Interests

Both authors have acted as independent consultants for a variety of organisations including hydrocarbon operating companies and governmental organisations on issues pertaining to induced seismicity. Both authors have been retained to provide seismic hazard assessments for companies who are currently applying for licences to conduct hydraulic fracturing in shallow formations in the WCSB.

Acknowledgements

We would like to thank Editor-in-Chief Thomas Pratt, Associate Editor Cezar Trifu, and Delphine Fitzenz and two anonymous reviewers for their constructive comments, which helped improve the quality of this article.

References

Anderson, Z. and D. Eaton, 2016. Induced seismicity due to wastewater injection near Peace River, Alberta: Geoconvention Conference, Calgary AB.

Arndt, K.K., 2017. Reservoir characterization and prediction of the lower Cretaceous Glauconite Member at Jenner-Suffield field, Alberta, Canada: M.Sc Thesis, Baylor University.

Baisch, S., C. Koch, A. Muntendam-Bos, 2019. Traffic light systems: To what extent can induced seismicity be controlled: Seismological Research Letters 90, 1145-1154.

Bao, X. and D.W. Eaton, 2016. Fault activation by hydraulic fracturing in western Canada: Science 354, 1406-1409.

Baranova, V., A. Mustaqeem, S. Bell, 1999. A model for induced seismicity caused by hydrocarbon production in the Western Canada Sedimentary Basin: Canadian Journal of Earth Sciences 36, 47-64.

Cesca, S., A. Rohr, T. Dahm, 2012. Discrimination of induced seismicity by full moment tensor inversion and decomposition: Journal of Seismology 17, 147-163.

Chalmers, G.R.L., R.M. Bustin, A.A.M. Bustin, 2012a. Geological controls on matrix permeability of the Doig-Montney hybrid shale-gas–tight-gas reservoir, northeastern British Columbia: Geoscience BC, Report 2012-1, 87-96.

Chalmers, G.R.L., D.J.K. Ross, R.M. Bustin, 2012b. Geological controls on matrix permeability of Devonian gas shales in the Horn River and Liard basins, northeastern British Columbia, Canada: International Journal of Coal Geology 103, 120- 131.

Clarke, H., L. Eisner, P. Styles, P. Turner, 2014. Felt seismicity associated with shale gas hydraulic fracturing: The first documented example in Europe: Geophysical Research Letters 41, 8308-8314.

Clarke, H., J.P. Verdon, T. Kettlety, A.F. Baird, J-M. Kendall, 2019. Real time imaging, forecasting and management of human-induced seismicity at Preston New Road, Lancashire, England: Seismological Research Letters 90, 1902-1915.

Cui, X. and B. Nassichuk, 2018. Permeability of the Montney Formation in the Western Canada Sedimentary Basin: insights from different laboratory measurements: Bulletin of Canadian Petroleum Geology 66, 394-424.

Dahm, T., D. Becker, M. Bischoff, S. Cesca, B. Dost, R. Fritschen, S. Hainzl, C.D. Klose, D. Kühn, S. Lasocki, Th. Meier, M. Ohrnberger, E. Rivalta, U. Wegler, S. Husen, 2013. Recommendation for the discrimination of human-related and natural seismicity: Journal of Seismology 17, 197-202.

Dahm, T., S. Cesca, S. Hainzl, T. Braun, F. Krüger, 2015. Discrimination between induced, triggered, and natural earthquakes close to hydrocarbon reservoirs: A probabilistic approach based on the modeling of depletion-induced stress changes and seismological source parameters: Journal of Geophysical Research, 120, 2491-2509.

Davis, S.D. and C. Frohlich, 1993. Did (or will) fluid injection cause earthquakes? Criteria for a rational assessment: Seismological Research Letters 64, 207-224.

Davis, S.D., P.A. Nyffenegger, C. Frohlich, 1995. The 9 April 1993 earthquake in south-central Texas: was it induced by fluid withdrawal? Bulletin of the Seismological Society of America 85, 1888-1895.

Eaton, D.W. and N. Igonin, 2018. What controls the maximum magnitude of injection-induced earthquakes? The Leading Edge 37, 135-140.

Eaton, D.W. and R. Schultz, 2018. Increased likelihood of induced seismicity in highly overpressured shale formations: Geophysical Journal International 214, 751-757.

Eaton, D.W., N. Igonin, A. Poulin, R. Weir, H. Zhang, S. Pellegrino, G. Rodriguez, 2018. Induced seismicity characterization during hydraulic-fracture monitoring with a shallow-wellbore geophone array and broadband sensors: Seismological Research Letters 89, 1641-1651.

Eyre, T.S., D.W. Eaton, M. Zecevic, D. D'Amico, D. Kolos, 2019. Microseismicity reveals fault activation before M_W 4.1 hydraulic-fracturing induced earthquake: Geophysical Journal International 218, 534-546.

Farahbod, A.M., H. Kao, D.M. Walker, J.F. Cassidy, 2015. Investigation of regional seismicity before and after hydraulic fracturing in the Horn River Basin, northeast British Columbia: Canadian Journal of Earth Sciences 52: 112-122.

Foulger, G. R., M.P. Wilson, J.G. Gluyas, B.R. Julian, R.J. Davies, 2018. Global review of human-induced earthquakes: Earth Science Reviews 178, 438-514.

Friesen, O.J., S.E. Dashtgard, J. Miller L. Schmitt, C. Baldwin, 2017. Permeability heterogeneity in bioturbated sediments and implications for waterflooding of tight-oil reservoirs, Cardium Formation, Pembina Field, Alberta, Canada: Marine and Petroleum Geology 82, 371-387.

Frohlich, C., H. DeShon, B. Stump, C. Hayward, M. Hornbach, J.I. Walter, 2016. A historical review of induced earthquakes in Texas: Seismological Research Letters 87, 1022-1038.

Ghanbari, A., S.M. Werner, L. Sadownyk, M. Gonzalez, P.K. Pedersen, 2019. Characterization and evaluation of deltaic sandstone reservoirs of the Dunvegan Formation, Kaybob South: Core Conference, AER Core Research Centre, May 2019.

Ghanizadeh A., C.R. Clarkson, A. Vahedian, O.H. Ardakani, J.M. Wood, H. Sanei, 2018. Laboratory-based characterization of pore network and matrix permeability in the Montney Formation: Insights from methodology comparisons: Bulletin of Canadian Petroleum Geology 66, 472-498.

Ghofrani H. and G.M. Atkinson, 2020. Activation rate of seismicity for hydraulic fracture wells in the Western Canada sedimentary basin: Bulletin of the Seismological Society of America 110(5), 2252-2271.

Hosseini, B.K. and D.W. Eaton, 2018. Fluid flow and thermal modeling for tracking induced seismicity near the Graham disposal well, British Columbia (Canada): SEG 88th Annual Conference, Anaheim CA, Expanded Abstracts 4987-4991.

Kettlety T., J.P. Verdon, M.J. Werner, J-M. Kendall, J. Budge, 2019. Investigating the role of elastostatic stress transfer during hydraulic fracturing-induced fault activation: Geophysical Journal International 217, 1200-1216

Kettlety T., J.P. Verdon, M. Werner, J-M. Kendall, 2020a. Stress transfer from opening hydraulic fractures controls the distribution of induced seismicity: Journal of Geophysical Research 125, e2019JB018794

Kettlety T., J.P. Verdon, M. Hampson, L. Craddock, 2020b. The M_L 2.9 August 2019 earthquake in Lancashire, UK, induced by hydraulic fracturing during Preston New Road PNR-2 operations: Seismological Research Letters, DOI: 10.1785/0220200187.

McGarr, A., 2014. Maximum magnitude earthquakes induced by fluid injection: Journal of Geophysical Research 119, 1008-1019.

Mossop, G.D. and I. Shetsen, 1994. Geological atlas of the Western Canada Sedimentary Basin: Canadian Society of Petroleum Geologists and Alberta Research Council. Available at https://ags.aer.ca/reports/atlas-of-the-western- canada-sedimentary-basin.htm

Mustanen, D., J Fianu, J. Pucknell, 2017. Account of hydraulically fractured onshore wells in the UK and seismicity associated with these wells: Journal of Petroleum Science and Engineering 158, 202-221.

National Research Council, 2013. Induced seismicity potential in energy technologies. The National Academies Press, Washington D.C., 300 pp.

Passarelli, L., F. Maccaferri, E. Rivalta, T. Dahm, E. Abebe Boku, 2013. A probabilistic approach for the classification of earthquakes as ‘triggered’ or ‘not triggered’: Journal of Seismology 17, 165-187.

Pawley, S., R. Schultz, T. Playter, H. Corlett, T. Shipman, S. Lyster, T. Hauck, 2018. The geological susceptibility of induced earthquakes in the Duvernay play: Geophysical Research Letters 45, 1786-1793.

Peña-Castro, A.F., M.P. Roth, A. Verdecchia, J. Onwuemeka, Y. Liu, R.M. Harrington, Y. Zhang, H. Kao, 2020. Stress chatter via fluid flow and fault slip in a hydraulic fracturing induced earthquake sequence in the Montney formation, British Columbia: Geophysical Research Letters 47, e2020GL087254.

Riazi, N., D. Eaton, A. Aklilu, 2020. Novel methods for characterizing induced seismicity in the Montney Formation, British Colombia, Canada: 82nd EAGE Annual Conference Expanded Abstracts, Th_E106_03.

Ross, G.M., and D.W. Eaton, 1999. Basement reactivation in the Alberta Basin: Observational constraints and mechanical rationale: Bulletin of Canadian Petroleum Geology 47, 391-411.

Roth, M.P., A. Verdecchia, R.M. Harrington, Y. Liu, 2020. High-resolution imaging of hydraulic fracturing-induced earthquake clusters in the Dawson-Septimus area, northeast British Columbia, Canada: Seismological Research Letters 91, 2744-2756.

Schoenball, M., N.C. Davatzes, J.M.G. Glen, 2015. Differentiating induced and natural seismicity using space-time-magnitude statistics applied to the Coso Geothermal field: Geophysical Research Letters 42, 6221-6228.

Schultz, R. and R. Wang, 2020. Newly emerging cases of hydraulic fracturing induced seismicity in the Duvernay East shale basin: Tectonophysics 779, 228393.

Schultz, R., V. Stern, Y.J. Gu, 2014. An investigation of seismicity clustered near the Cordel Field, west central Alberta, and its relation to a nearby disposal well: Journal of Geophysical Research 119, 3410-3423.

Schultz, R., V. Stern, Y.J. Gu, D. Eaton, 2015. Detection threshold and location resolution of the Alberta Geological Survey earthquake catalogue: Seismological Research Letters 86, 385-397.

Schultz, R., G. Atkinson, D.W. Eaton, Y.J. Gu, and H. Kao, 2018. Hydraulic fracturing volume is associated with induced earthquake productivity in the Duvernay play: Science 359, 304-308.

Shapiro, S.A., C. Dinske, C. Langenbruch, 2010. Seismogenic index and magnitude probability of earthquakes induced during reservoir fluid stimulations: The Leading Edge 29, 304-309.

Skoumal, R.J., M.R. Brudzinski, B.S. Currie, 2018. Proximity of Precambrian basement affects the likelihood of induced seismicity in the Appalachian, Illinois, and Williston basins, central and eastern United States: Geosphere 14, 1365-1379.

Verdon, J.P. and J. Budge, 2018. Examining the capability of statistical models to mitigate induced seismicity during hydraulic fracturing of shale gas reservoirs: Bulletin of the Seismological Society of America 108, 690-701.

Verdon, J.P. and J.J. Bommer, 2021. Green, yellow, red, or out of the blue? An assessment of Traffic Light Schemes to mitigate the impact of hydraulic fracturing-induced seismicity: Journal of Seismology 25, 301-326.

Verdon J.P., B.J. Baptie, J.J. Bommer, 2019a. An improved framework for discriminating seismicity induced by industrial activities from natural earthquakes: Seismological Research Letters 90, 1592-1611.

Verdon, J.P., N. Igonin, J-M. Kendall, D.W. Eaton, 2019b. Fault reactivation via pre-existing fracture networks during hydraulic fracturing: Society of Earthquake and Civil Engineering Dynamics Conference, Greenwich London, Conference Proceedings 7.4.

Wetmiller, R.J., 1986. Earthquakes near Rocky Mountain House, Alberta, and their relationship to gas production facilities: Canadian Journal of Earth Sciences 23, 172-181.

Yassin, M.R., M. Begum, H. Dehghanpour, 2017. Organic shale wettability and its relationship to other petrophysical properties: a Duvernay case study: International Journal of Coal Geology 169, 74-91.

APPENDIX A: CASE-BY-CASE EVALUATION OF TABLE 1 EVENTS

Berland River: 2009-08-10 M 3.0

A single event near to Berland River, to the south of Fox Creek, is linked by the GA20 method with 5 co-located wells that target Mannville (Wilrich, 100/07-18-057-23W5/03; Gething, 100/07-18-057-23W5/02; Notikewin, 100/07-18-057-23W5/04), Colorado (100/07-18-057-23W5/06) and Dunvegan (100/07-18-057-23W5/05) formations.

Figure A-1 shows a map of this event, and its relationship to adjacent oil and gas activities. The Mannville/Colorado/Dunvegan wells are 17.4 km from the event and were stimulated by < 300 m^3 of fluid each, between 04/08/2009 – 05/08/2009, 5 days before the event occurred. The largest W value for these wells is 0.55. Worldwide, we are not aware of any cases of HF-IS being generated from injection of such small volumes of fluid. Given the very low volumes involved with these stimulations – 2 orders of magnitude lower than the volumes typically associated with stimulation of the Duvernay and Montney, for example – any perturbation that they could cause would be limited to very close to the well. A location uncertainty that is significantly larger than that estimated by Schultz et al. (2015), and larger even than the 10 km location uncertainty adopted by GA20, would be required to co-locate this event the Mannville/Colorado/Dunvegan wells.

There are two high volume injection wells that could present a more plausible potential cause for this event than the stimulated wells, given that these disposal wells have injected 3.5 orders of magnitude more fluid. These wells target the Devonian-age Leduc formation. However, since this is a single, isolated event, and that three events of similar magnitude have been observed in this area between 1960 – 2000, prior to the onset of HF activities, it is more likely that this is a natural event. A large number of stimulated wells are present in the area. None of the other 500 Cretaceous wells in the area, most of which were stimulated between 2004 to 2012, are linked to any earthquakes. We note that a burst of seismicity begins in late 2014, which appears to correspond with the onset of hydraulic fracturing in the underlying Montney formation.

Given the low volumes of fluid used to stimulate the identified wells, and the distances between the identified wells and the event, it is implausible that the 2009 event was triggered by activities in the wells to which the GA20 method has linked it.

Wolf Lake: 08/10/2010 M 3.2

This earthquake is located to the northwest of the Brazeau Reservoir. It was linked by the GA20 method to a well in the Mannville Formation, with W = 0.55. Figure A-2 shows a map of this event, and its relationship to adjacent oil and gas activities.

The Mannville well (100/13-13-050-15W5/00) was stimulated on 05/10/2010, 3 days before the event. However, this well is 20.0 km from the event location. Event location uncertainties far higher than those estimated by Schultz et al. (2015), and those adopted by GA20, would be required to co-locate this event with the identified Mannville well. The event is too far from the well for hydraulic fracturing, using a volume of ~ 600 m^3 (the volume injected by this well), to be considered to be a plausible cause.

There are 4 high-volume water disposal wells in the area, the largest of which has injected over 2 million m^3 since 1990. These wells target the Devonian-age Nisku Formation. It is possible that this event has a natural origin, and it is also possible that these disposal wells may have caused the identified event, especially since 3 other earthquakes have occurred in the vicinity of these disposal wells while they have

been active. In contrast, any link with the identified Mannville well is clearly spurious, and it is again apparent that the association of the 08/10/2010 event with this well by the GA20 method is not plausible.

Fox Creek Duvernay: 15/01/2015 M3.3

This earthquake is located in the Fox Creek region, where seismicity has been induced by stimulation of the Duvernay Formation (e.g., Bao and Eaton, 2016). A map and timeline of these event and nearby oil and gas activities is shown in Figure A-3.

The event was linked by the GA20 method (W = 0.55) to hydraulic fracturing in one Dunvegan well (100/05-13-062-26W5/00). This well injected approximately 3,000 m^3 of fluid, taking one day to complete, on 11/1/2015, 4 days before the occurrence of the associated event. However, the Dunvegan well is located over 19 km from the event, and so a very large location error would be required to co-locate this event with the associated Dunvegan well.

This event has a much stronger link to a Duvernay well (W = 0.85) that was active at the time (100/15-15-062-23W5/02). The Duvernay well injected approximately 26,000 m^3 and was active from 11/1/2015 to 20/1/2015. The identified event is part of a cluster of M < 3 events that occurred during stimulation of the Duvernay well. The identified event is located approximately 4 km from the toe of the Duvernay well, but given a reasonable location uncertainty of 3 km (based on Schultz et al., 2015), the event could be within 1 km of the well.

We note that in Table A1 of GA20, the Reference ID notes for this case identify this as one of the earthquakes studied by Bao and Eaton (2016), who explicitly linked this event, and other clusters of seismicity in the area, to hydraulic fracturing of the Duvernay. It is clear that this event has been induced by stimulation of the Duvernay, and that any links to the Dunvegan well are not plausible.

Fox Creek Duvernay, 16/01/2017 M 3.0

Much like the previous example, this earthquake is located in the Fox Creek region, where HF-IS caused by stimulation of the Duvernay Formation is extensively documents. This event was linked by the GA20 method (W = 0.36) to hydraulic fracturing in a Dunvegan well (100/04-13-062-26W5/00,. This well injected approximately 4,000 m^3 of fluid, taking one day to complete, on 5/1/2017 (10 days before the occurrence of the identified event). This well is located over 10 km from the event location. Figure A-4 shows a map and timeline of this case.

Much like the previous case, this event has a much stronger link (W = 1.0) to four Duvernay wells that were also active at the time (100/05-25-061-25W5/00, 100/11-25-061-25W5/00, 100/10-25-061-25W5/00, 100/06-25-061-25W5/00). These Duvernay wells all injected approximately 40,000 m^3, and began operations on 5/1/2017, and were still undergoing stimulation when the identified event occurred. The event location is co-located with the subsurface tracks of the Duvernay wells, and is part of a sequence of M < 3.0 events that occurred around these Duvernay wells, which began at the same time that the Duvernay wells became active. As such, the link between these events and the Duvernay wells is clear and obvious, and it is equally clear that the association produced by the GA20 method between this event and the Dunvegan wells is not plausible.

Tables

Table 1: Listing of all events and associated Cretaceous wells with $W \geq 0.35$

Event Date/Time	Magnitude	Lat	Lon	Well UWI/Formation	W	Well-event distance [km]	Lag [days]
2009-08-10 02:38:46	3.0	54.07	-117.49	100/07-18-057-23W5/03 Mannville	0.49	17.4	6
⋮	⋮	⋮	⋮	100/07-18-057-23W5/02 Mannville	0.49	17.4	6
⋮	⋮	⋮	⋮	100/07-18-057-23W5/04 Mannville	0.55	17.4	5
⋮	⋮	⋮	⋮	100/07-18-057-23W5/05 Dunvegan	0.55	17.4	5
⋮	⋮	⋮	⋮	100/07-18-057-23W5/06 Colorado	0.55	17.4	5
2010-10-08 20:14:24	3.2	53.12	-116.02	100/13-13-050-15W5/00 Mannville	0.55	20.0	4
2013-01-01 01:01:00	3.0	52.81	-116.11	102/10-09-044-15W5/00 Cardium	0.57	2.9	62
2015-01-15 19:18:29	3.3	54.38	-117.46	100/05-13-062-26W5/00 Dunvegan	0.55	19.1	5
2017-01-16 02:22:36	3.0	54.31	-117.59	100/04-13-062-26W5/00 Dunvegan	0.36	11.54	11
2017-12-05 16:01:22	3.1	54.23	-116.63	100/12-18-060-17W5/00 Cardium	0.46	8.8	8
⋮	⋮	⋮	⋮	100/05-05-061-18W5/00 Dunvegan	0.68	1.8	18
⋮	⋮	⋮	⋮	100/13-32-060-18W5/00 Dunvegan	0.68	1.8	19
⋮	⋮	⋮	⋮	102/03-26-060-18W5/00 Dunvegan	0.59	2.0	47
2017-12-07 13:28:29	3.1	54.24	-116.64	100/12-18-060-17W5/00 Cardium	0.39	10.4	11
⋮	⋮	⋮	⋮	100/05-05-061-18W5/00 Dunvegan	0.67	0.8	20
⋮	⋮	⋮	⋮	100/13-32-060-18W5/00 Dunvegan	0.66	0.8	21
⋮	⋮	⋮	⋮	102/03-26-060-18W5/00 Dunvegan	0.58	2.9	49
2017-12-16 01:13:36	3.4	54.24	-116.64	100/05-05-061-18W5/00 Dunvegan	0.63	1.0	28
⋮	⋮	⋮	⋮	100/13-32-060-18W5/00 Dunvegan	0.62	1.0	29
⋮	⋮	⋮	⋮	102/03-26-060-18W5/00 Dunvegan	0.57	2.4	57
⋮	⋮	⋮	⋮	100/04-08-060-17W5/00 Dunvegan	0.60	11.5	2
⋮	⋮	⋮	⋮	100/05-08-060-17W5/00 Dunvegan	0.60	11.5	1
⋮	⋮	⋮	⋮	100/03-10-060-17W5/03 Viking	0.52	12.5	6
2019-03-10 10:00:36	3.8	52.57	-115.26	104/12-35-042-08W5/00 Cardium	0.42	18.8	7
⋮	⋮	⋮	⋮	102/13-35-042-08W5/02 Cardium	0.36	18.8	9

Figures

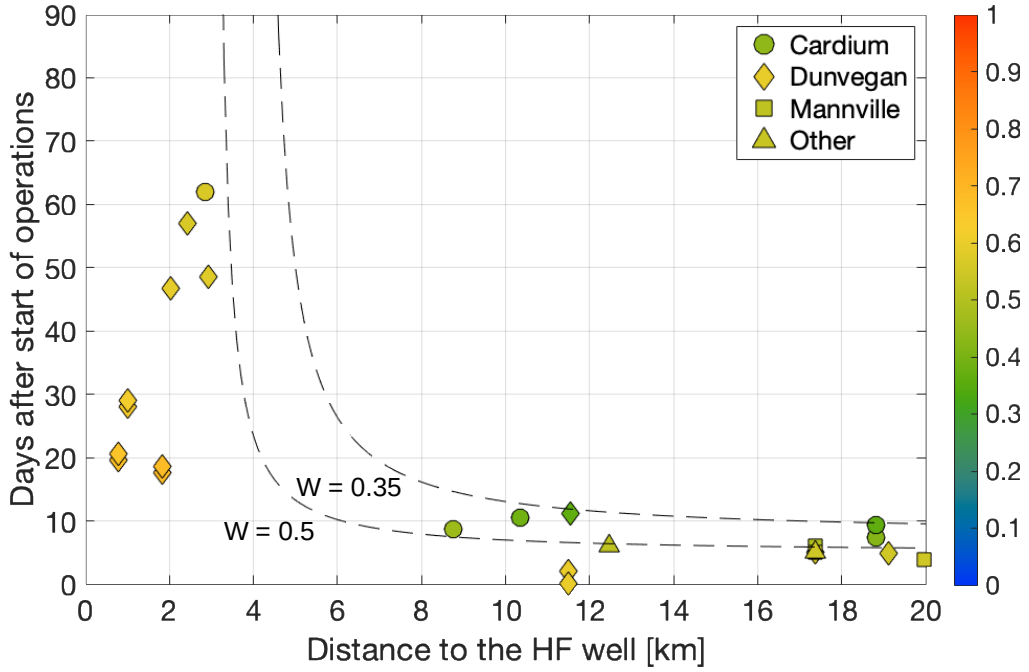

Figure 1: W values for all earthquakes with $W \geq 0.35$ for wells targeting Cretaceous-age strata, showing the distance between each well pad and event, and the time lag between the event and the start of operations. Symbol shapes represent different formations, and are colored by the W score.

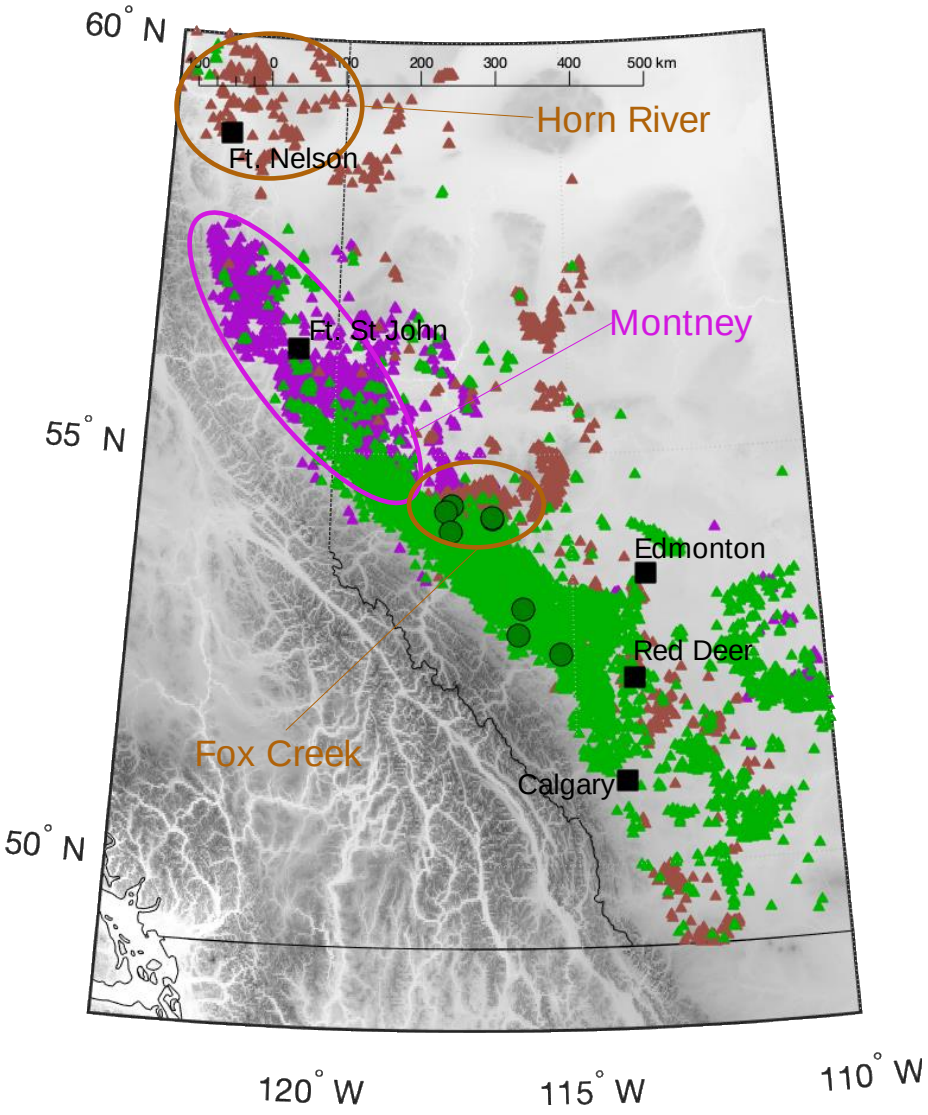

Figure 2: Map showing locations of earthquakes (green dots) from 2009 onwards, with $M \geq 3$, that are linked by the GA20 method to wells stimulating Cretaceous-age strata (with $W \geq 0.35$) . We also show all wells stimulated in Devonian-age (brown triangles), Triassic-age (purple triangles) and Cretaceous-age (green) formations. Three areas where cases of HF-IS have been prominent are marked: Horn River, where seismicity has been caused by operations in the Horn River Shale; the Montney trend; and Fox Creek, where seismicity has been caused by operations in the Duvernay Formation.

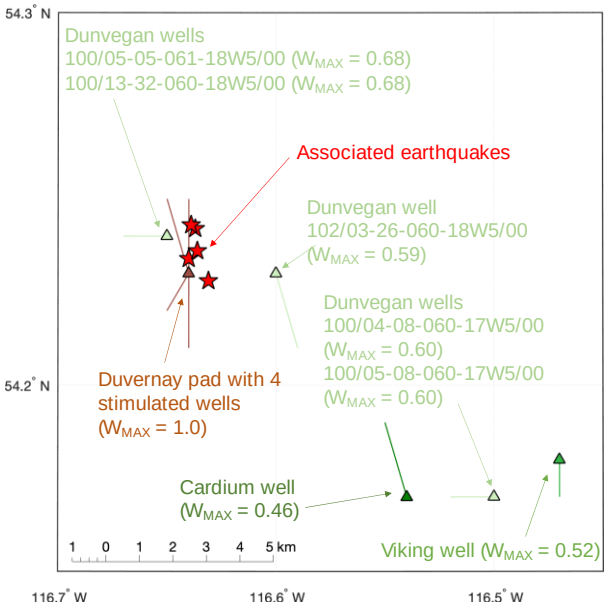

(a)

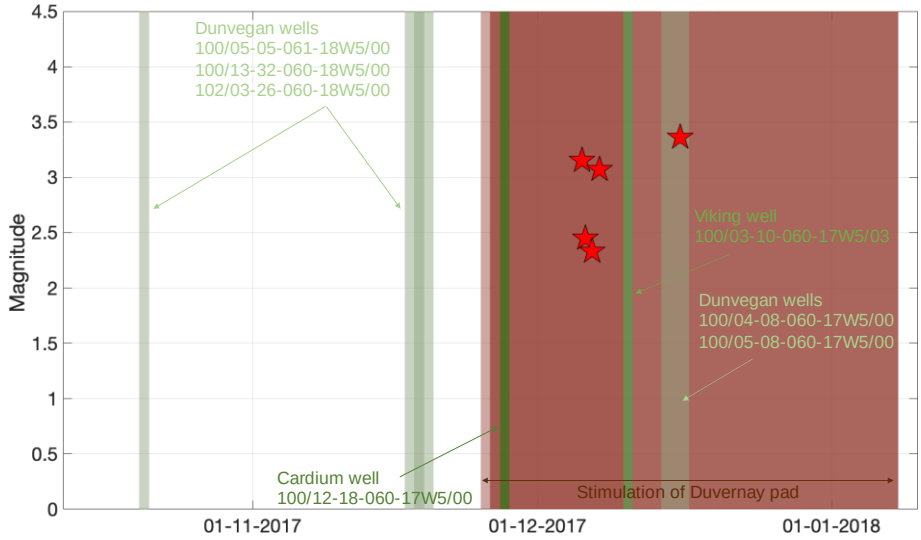

(b)

Figure 3: Map (a) and timeline (b) showing the 3 events occurring during December 2017 that were associated by the GA20 method with hydraulic fracturing in Cardium, Dunvegan, and Viking wells. The location of the Cardium well is shown by the dark green triangle (and lines showing the well track in the subsurface), and the locations of the Dunvegan wells by light green triangles and lines. Four Duvernay wells were also active at this time, shown by the brown diamond and lines. Five $M \geq 2.0$ earthquakes that occurred during the time of interest are shown as red stars. Maximum W values for each well (W_{MAX}) are also shown. In (b) we show the days in which HF took place in the Cardium (dark green), Dunvegan (light green), Viking (mid-green) and Duvernay (brown) wells, and the occurrence dates of the associated earthquakes.

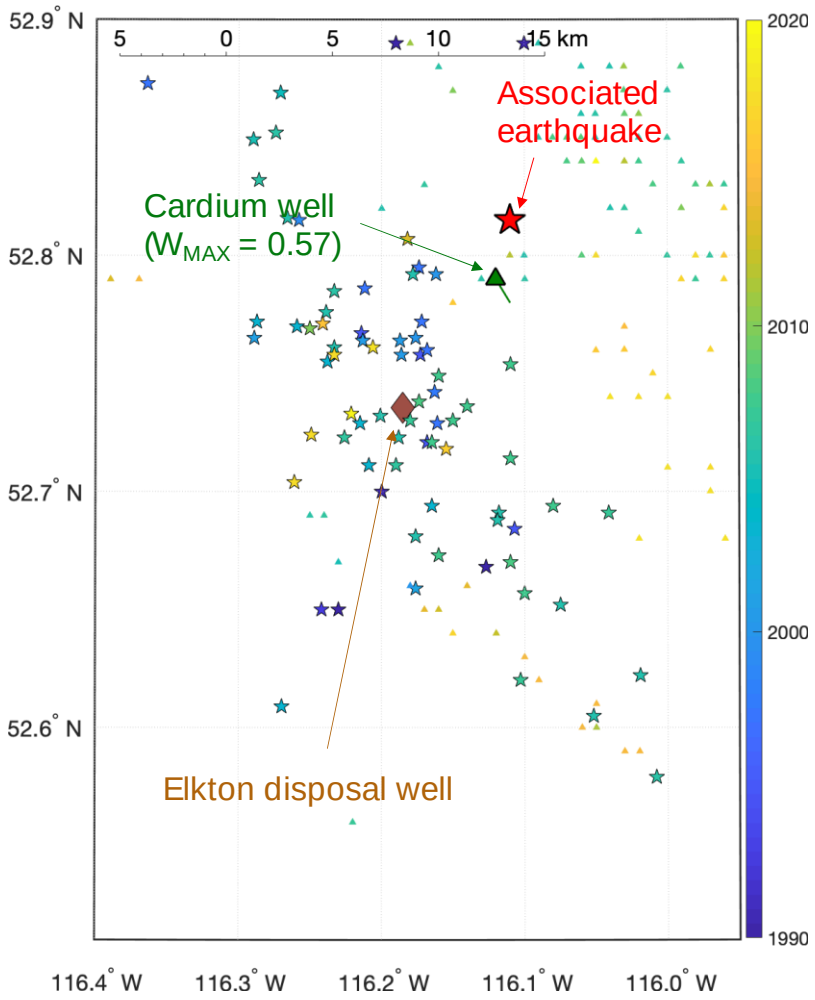

Figure 4: Map showing the event that occurred on 01/01/2013 in the Cordel cluster that was linked by the GA20 method with hydraulic fracturing in a Cardium well (dark green triangle). A high-volume disposal well targeting the Elkton Formation (Mississippian age) is marked by a brown diamond. Other stimulated wells (triangles) are also shown, coloured by the year in which stimulation took place. Stars show all $M \geq 2$ earthquakes coloured by their occurrence date – the event associated with the Cardium well is marked by a red star.

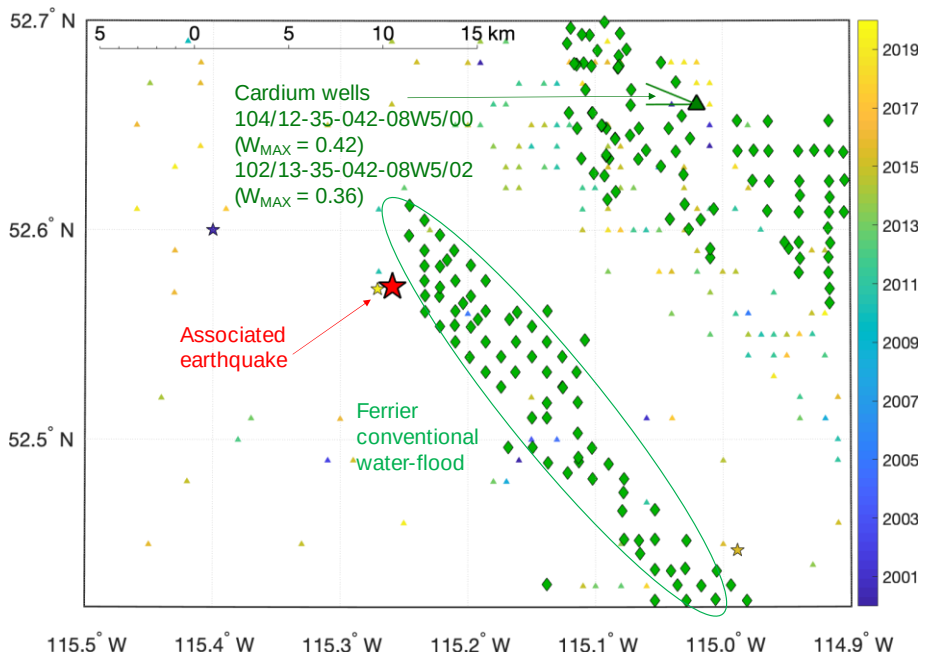

Figure 5: Map showing the event on 2019-03-10 (red star) that is linked by the GA20 method to two Cardium wells (green triangle, with lines marking the well track). The event is found near a swathe of injection wells (green diamonds) conducting a waterflood in the Ferrier field. Other earthquakes (stars) and hydraulic fracturing wells (triangles) are shown, coloured by their data of occurrence.

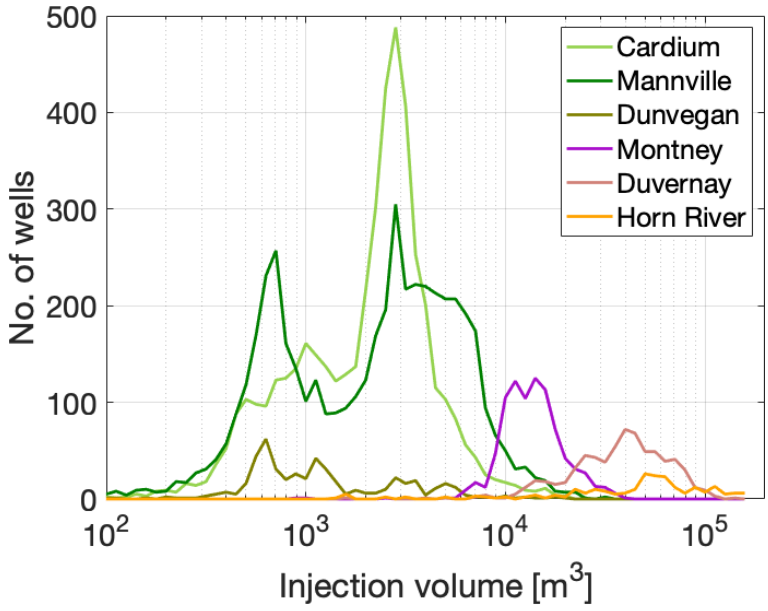

Figure 6: Injection volumes used per well for hydraulic fracturing in different formations in the WCSB.

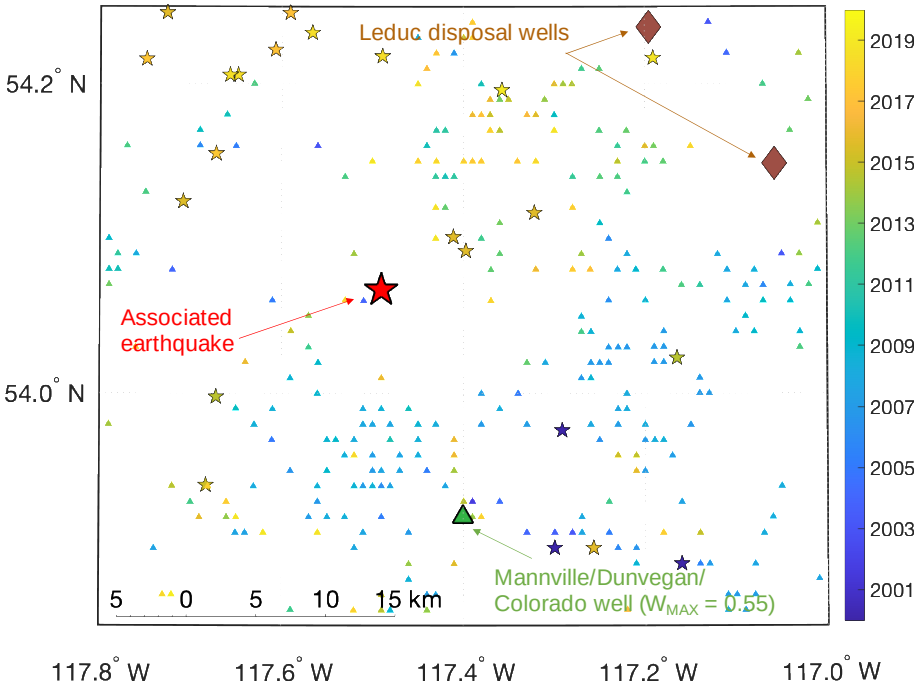

(a)

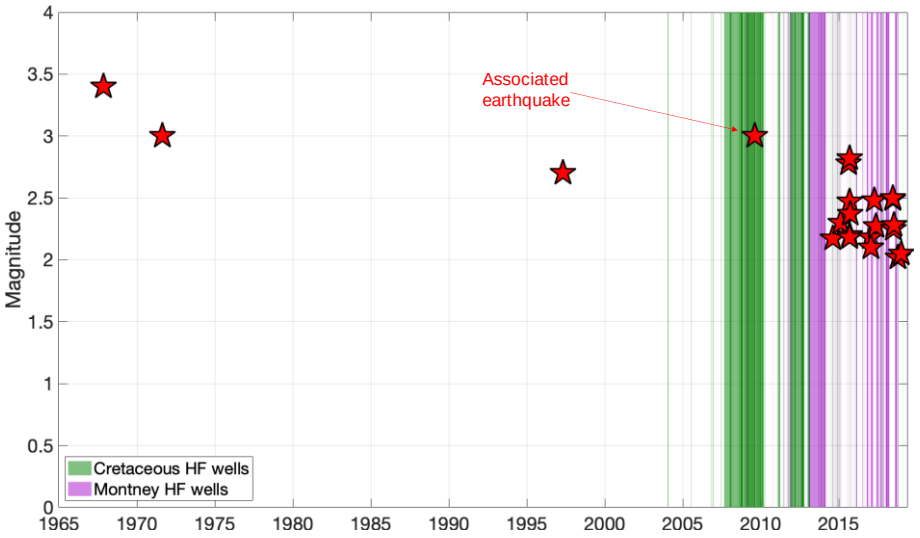

(b)

Figure A-1: Map (a) and timeline (b) showing the event that occurred on 10/08/2009 near to Berland River that was linked by the GA20 method with hydraulic fracturing in 5 co-located Mannville/Colorado/Dunvegan wells (light green triangle). Other hydraulic fracturing wells are shown (triangles), coloured by the year in which HF took place. Two nearby high-volume injection wells are also highlighted, which target the Leduc formation. Stars show all $M \geq 2$ earthquakes coloured by their occurrence date – the event linked to the Mannville wells is marked by a red star. In (b) we show a timeline of earthquakes in this area (stars), with green (Cretaceous wells) and purple (Montney wells) shading showing dates when hydraulic fracturing took place in the area.

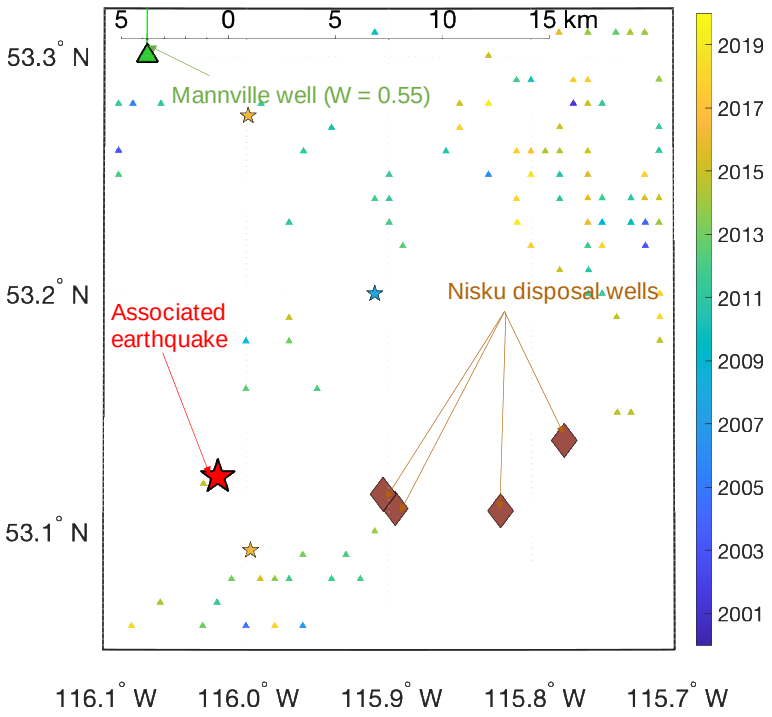

Figure A-2: Map showing the event that occurred on 08/10/2010 near to Wolf Lake that was linked by the GA20 method with hydraulic fracturing in a Mannville well (light green triangle with lines showing the well tracks in the subsurface). Four high-volume disposal wells targeting the Nisku Formation (Devonian age) are also marked by brown diamonds. Other stimulated wells (triangles) are also shown, coloured by the year in which stimulation took place. Stars show $M \geq 2$ earthquakes coloured by their occurrence date – the event associated with the Mannville well is marked by a red star.

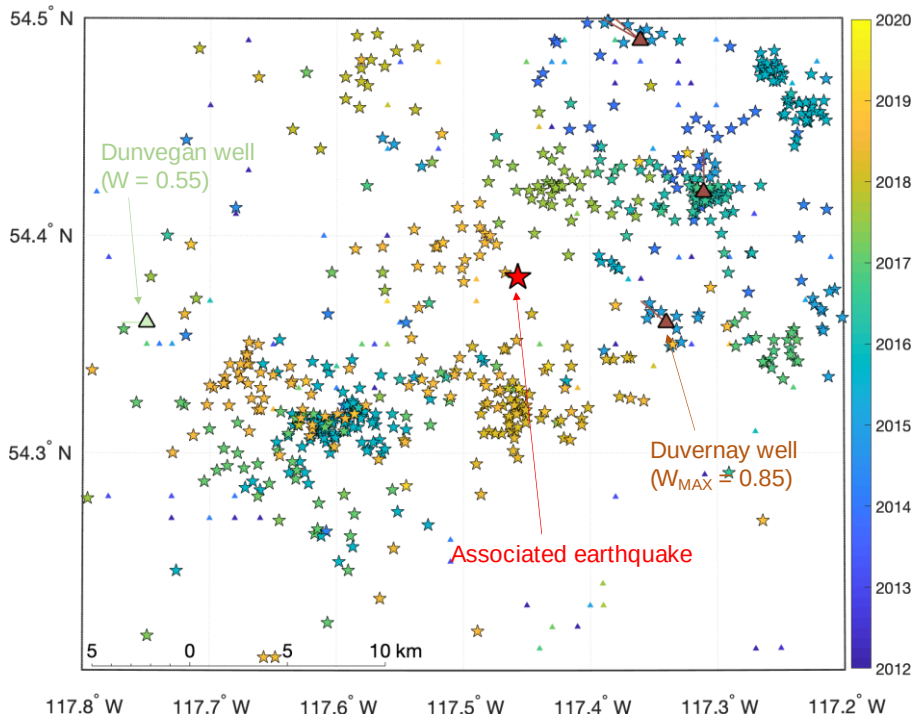

(a)

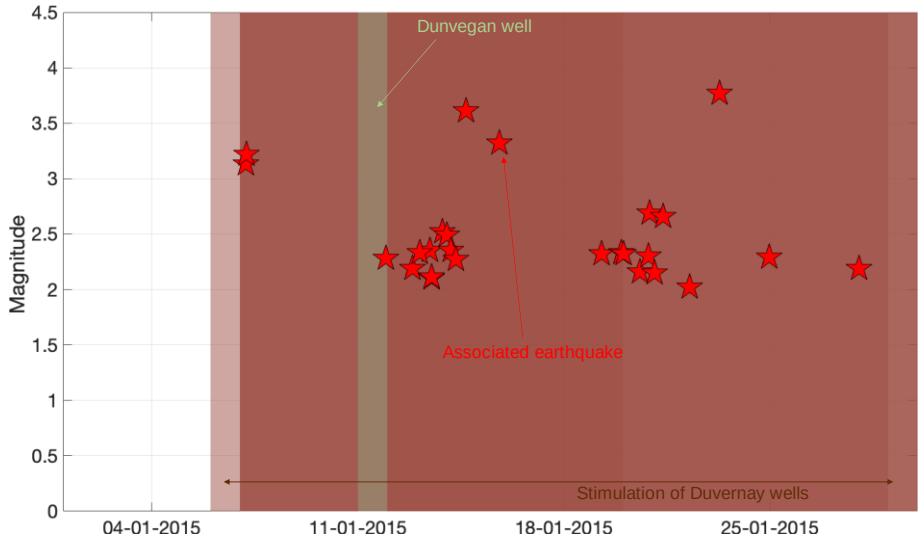

(b)

Figure A-3: Map (a) and timeline (b) showing the earthquake that occurred during January 2015 that was associated by the GA20 method with hydraulic fracturing in a Dunvegan well. In (a) the location of the Dunvegan well is shown by the light green triangle (and lines showing the well track in the subsurface), and the locations of several Duvernay wells that were also active at this time are shown as brown triangles. Other stimulated wells in the area are shown as triangles coloured by the date of stimulation. The identified earthquake is shown as a red star, and all other $M \geq 2$ earthquakes are shown as stars coloured by occurrence date. In (b) we show the days in which HF took place in the Dunvegan (light green) and Duvernay (brown) wells, and the occurrence dates of nearby earthquakes.

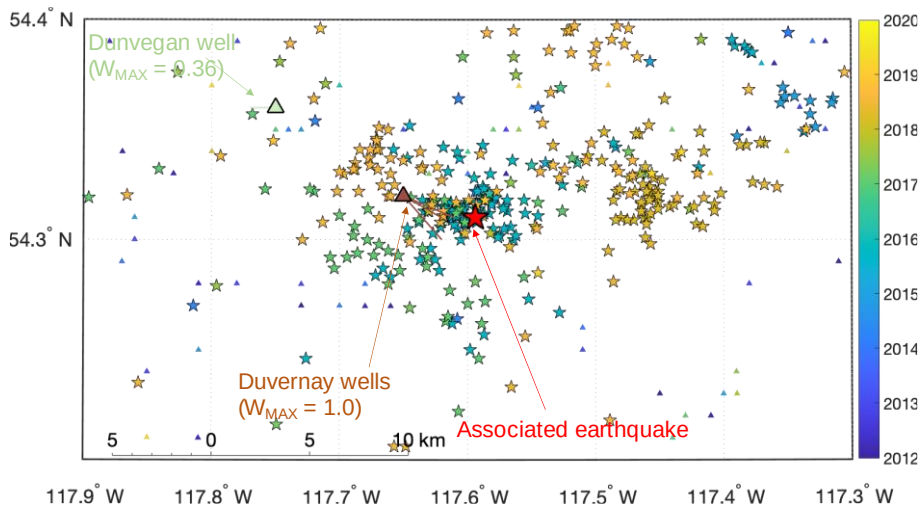

(a)

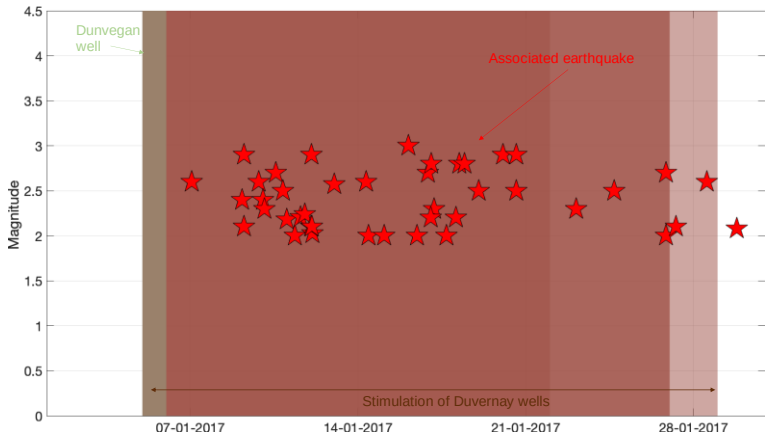

(b)

Figure A-4: Map (a) and timeline (b) showing the earthquake in January 2017 that was linked by the GA20 method to hydraulic fracturing in a Dunvegan well. In (a), the location of the Dunvegan well is shown by the light green triangle (and line showing the well track in the subsurface). Four Duvernay wells were also active at this time, shown by the brown triangle and lines. Other hydraulic fracturing wells present in the area are also shown, coloured by the date of stimulation. All $M \geq 2$ earthquakes are shown, coloured by their occurrence date – the event linked to the Dunvegan well is marked by a red star. In (b) we show the days in which stimulation took place in the Dunvegan (green) and Duvernay (brown) wells, and the occurrence dates of the nearby earthquakes.